Zoology 145 (2021) 125888

Contents lists available at ScienceDirect

Zoology

journal homepage: www.elsevier.com/locate/zool

Comparative biomechanics of hagfish skins: diversity in material, morphology, and movement

E.B. Lane Kennedy [a], Raj P. Patel [a], Crystina P. Perez [a], Benjamin L. Clubb [b], Theodore A. Uyeno [b], Andrew J. Clark [a,*]

[a] Department of Biology, College of Charleston, 66 George Street, Charleston, SC, 29424, USA
[b] Department of Biology, Valdosta State University, 1500 N Patterson Street, Valdosta, GA, 31698, USA

ARTICLE INFO

Keywords:
Eptatretus
Myxine
fish skin
knotting
biaxial testing

ABSTRACT

The baggy skins of hagfishes confer whole-body flexibility that enables these animals to tie themselves into knots without injury. The skin's looseness is produced by a subcutaneous blood sinus that decouples the skin and body core and permits the core to contort dramatically without loading the skin in tension or shear. Hagfish skin represents a biological composite material comparable in strength and stiffness to the conventionally taut skins of other fishes. However, our understanding of hagfish skin is restricted to only one of 78 species: The Pacific hagfish *Eptatretus stoutii*. To determine if other hagfish share similar characteristics with *E. stoutii*, we measured material properties and compared histological data sets from the skins of four hagfish species: *E. springeri, E. stoutii*, *Myxine glutinosa*, and *M. hubbsi*. We also compared these material properties data with skins from the American eel, *Anguilla rostrata*. We subjected skin samples from all species to uniaxial tensile tests in order to measure strength, stiffness, extensibility, and toughness of skins stretched along longitudinal and circumferential axes. We also used a series of equibiaxial tensile tests on skin samples from *E. stoutii*, *M. glutinosa*, and *A. rostrata* to measure stiffness of skins simultaneously strained along both axes. Significant results of uniaxial and biaxial tests show that the skins from *Eptatretus* are anisotropic, being stiffer in the longitudinal axis, and more extensible than the isotropic skins of *Myxine*. Skins of *A. rostrata* were stiffer in the circumferential axis and they were stronger, tougher, and stiffer than all hagfish skins examined. The skins of *Eptatretus* are histologically distinct from *Myxine* skins and possess arrays of fibers that stain like muscle. These interspecific differences across hagfish skins show a phylogenetic pattern with knotting kinematics and flexibility; both genera belong to distinct but major subfamilies within the Myxinidae, and *Eptatretus* is known for creating and manipulating a greater diversity of knotting styles than *Myxine*.

1. Introduction

Jawlessness is a primitive trait of the craniates that imposes constraints on prey capture. In contrast to gnathostomes, which grasp prey with opposable rigid elements (e.g. upper and lower jaws), hagfishes use protractible dental plates for procuring food items (Clark and Summers, 2007). Despite possessing formidable arrays of keratinous dentition that can be forcefully retracted, the dental plates function like a freely-moving lower jaw that lacks an opposable upper jaw against which they may efficiently press for maximum effect (Uyeno and Clark, 2015; Clark et al., 2016). To close the kinetic chain in this feeding system, a hagfish ties its body into a knot and uses the rigid, knotted portion of the body like upper jaws to oppose the retracting dental plates which function like lower jaws (Fig. 1A, B). Furthermore, the opposable knotted body and dental plates physically articulate with one another at the site of the retractor complex of the hagfish feeding apparatus; a cylindrical muscular hydrostat comprised of a three-dimensionally sophisticated arrangement of connective tissues and muscle fibers divided into three muscle groups (Clubb et al., 2019). When these muscles contract simultaneously, the retractor complex becomes a rigid supportive skeleton for the retractor muscles (Clark et al., 2010) while creating a compression-resistant joint between the teeth and opposing body (Clark and Uyeno, 2019). Thus, the summation of activities from the dentition, body, and feeding musculature effectively transforms the jawless feeding system of a hagfish into a true biting system. In addition to amplifying the forces applied by the dental plates (Clark and

* Corresponding author.
E-mail address: clarkaj@cofc.edu (A.J. Clark).

https://doi.org/10.1016/j.zool.2020.125888
Received 9 September 2019; Received in revised form 3 December 2020; Accepted 4 December 2020
Available online 7 December 2020

Summers, 2012), a hagfish uses its body knot for extracting live fossorial prey (observed in a species of *Neomyxine*; Zintzen et al., 2011), removing excess slime from the surface of the body (Jensen, 1966), and maneuvering to escape predators (Jensen, 1966; Haney et al., 2020).

Complex arrangements of body core musculature, elongate bodies devoid of vertebrae, and unusually loose-fitting skins of hagfishes are adaptations that allow the movements required for creating and manipulating body knots (Clark et al., 2016). The slack fit of hagfish skins results from two novel morphologies: 1) a prominent, low-pressure subcutaneous venous blood sinus situated between the skin and the body core containing the axial muscles, viscera, notochord and spinal cord (Forster et al., 1989, 1991) and 2) a near absence of myoseptal-skin connections (Vogel and Gemballa, 2000) that create a strong mechanical linkage between body and the tight-fitting skin of most fish (Fig. 1C). The bagginess of the skin has recently been hypothesized to enhance the range of movement and flexibility of the decoupled body core (Clark et al., 2016; Uyeno and Clark, 2020), which can benefit hagfishes in many biologically relevant situations that include escaping predatory bites (Boggett et al., 2017), maneuvering through confined spaces (Freedman and Fudge, 2017), and manipulating body knots (Clark et al., 2016). Knots tied in a long thin cylinder of homogeneous composition involves concomitant bending and twisting that apply a complex combination of tension, shear, and compression to the cylinder's core and skin (Vogel, 2013). In hagfishes, however, these stresses on the skin and core are separated by the subcutaneous sinus, which provides space for the core to contort as needed without suddenly loading the skin in tension or shear. To limit further deformation when put in tension, cross-helical arrangements of tissue fibers within their skin may control the body's cross-sectional area during knot-driven pressurization and prevent the body from kinking during bending (Clark and Cowey, 1958).

Baggy skins could theoretically be inefficient for hagfishes because the subcutaneous sinus disrupts the force generated by the core musculature from being transferred to the skin. The increased drag incurred by decoupling the skin from the body core may be the price that hagfishes pay for being able to flexibly contort their bodies into a variety of knots. However, despite their minimal contribution to steady swimming movements (Long et al., 2002), the slack skins of hagfish are comparable in strength and stiffness to the taut skins of lampreys, bony fishes, and cartilaginous fishes (Clark et al., 2016). Similar to the skins of other fishes, the skins of the Pacific hagfish *Eptatretus stoutii* (Lockington, 1878) are anisotropic biological composites consisting of a fibrous dermis layer sandwiched between a superficial epidermis and a deep, fatty hypodermis (Welsch et al., 1998; Clark et al., 2016).

In most species of fishes, the taut skins serve as mechanical links between the core muscles and the propulsive surfaces of the body (Kenaley et al., 2018). Furthermore, the taut body coverings of some worms and fishes are highly effective at retaining body shape and also possess cross-helical arrays of fibers that limit excessive body shape deformations induced by increased internal pressures (Clark and Cowey, 1958). Restricted core movements and the tautness of many fish skins

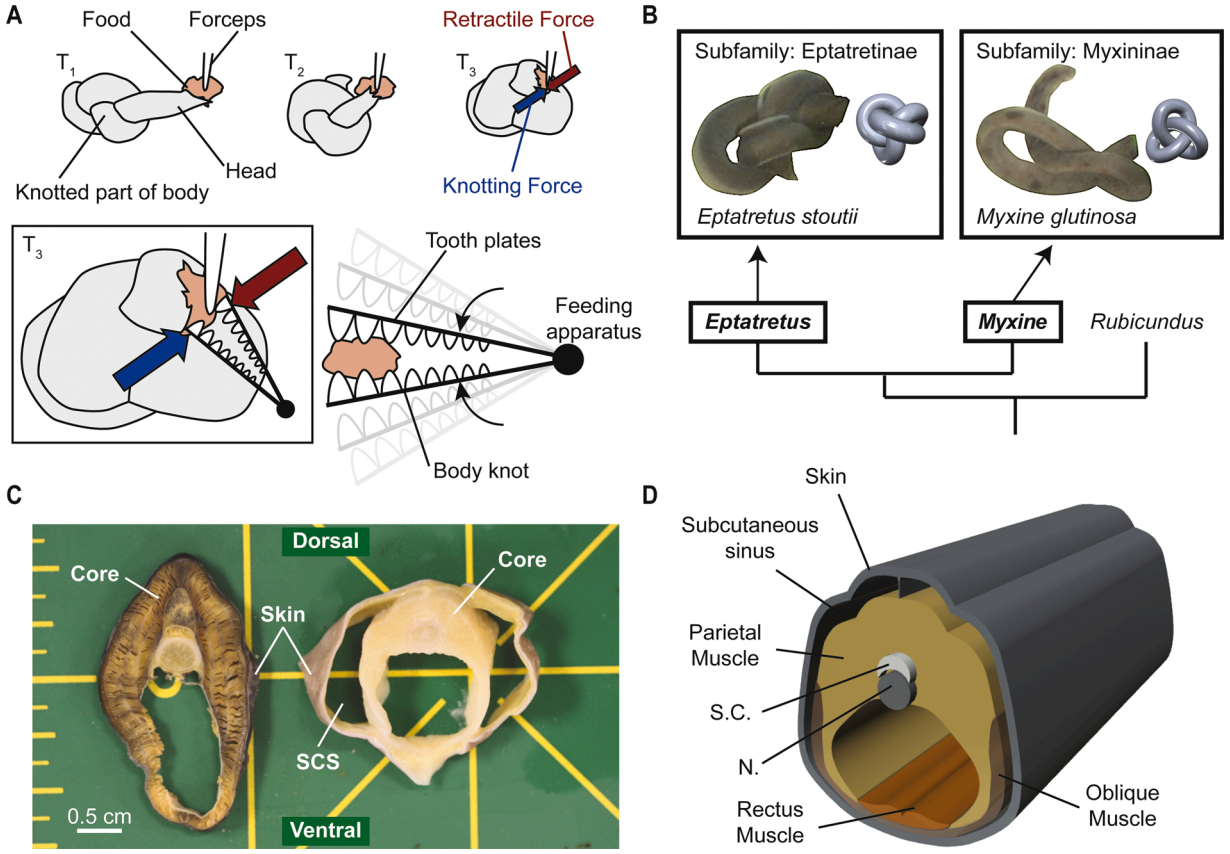

Fig. 1. Hagfish knotting behavior and adaptations for knotting. (A) Top: sequence of images showing how the rigid knotted part of the body slides over the head to apply an opposing force to the force generated by the dental plates. Bottom: the knot-assisted jawless feeding mechanism can be represented by simple drawings of upper and lower jaws joined posteriorly at a joint. These images were modified from Clark and Uyeno, 2019. (B) Top: video images of a Pacific hagfish *Eptatretus stoutii* (left) and an Atlantic hagfish *Myxine glutinosa* creating and manipulating body knots to extricate themselves from custom restraint devices. Photo credits: Haney et al., 2020. To the right of each animal, is a three-dimensional drawing of the knot style (figure eight or trefoil) readily produced by that lineage of hagfishes. Bottom: a summarized phylogeny of the extant hagfishes based on three genera. Each genus represents one of three subfamilies. (C) Photograph of transverse sections of a sea lamprey *Petromyzon marinus* (left) and the hagfish *M. hubbsi* (right) at approximately 50%*TL* to illustrate the loose connection between the skin and body core muscles in the hagfish. (D) Three-dimensional drawing illustrating the arrangements of three different groups of muscles comprising the body core. N., notochord; S. C., spinal cord.

can streamline the body, minimize drag, and in some species, the skins may function like external tendons, cyclically storing and releasing strain energy to facilitate oscillations of the body during steady swimming (Wainwright et al., 1978; Hebrank, 1980). Under tension, these tight-fitting skins are usually twice as stiff in the circumferential axis than in the longitudinal axis of the body, however, the loose-fitting skins of *E. stoutii* are nearly twice as stiff in the longitudinal axis than in the circumferential axis (Clark et al., 2016).

Even though the striking differences previously shown in the morphology and material properties of hagfish skins relative to those of other fishes have suggested the possible adaptation for knot-tying and maneuverability (Clark et al., 2016), this conclusion is based on an examination of one species. There are 78 species of hagfishes and approximately 90% of them belong to one of two major subfamilies: the Eptatretinae and the Myxininae (Fernholm et al., 2013; Fig. 1B). The kinematics of knotting, and the styles of knots created, can vary across species of hagfish (Haney et al., 2020). In laboratory settings, specimens of the Myxinine, *Myxine glutinosa* (Linnaeus, 1758), exclusively tie their bodies into overhand knots (Fig. 1B), while Eptatretines, like *E. stoutii* (Lockington, 1878) and *E. springeri* (Bigelow & Schroeder, 1952), execute more complex knots in addition to overhand knots, such as figure-of-eight knots and three-twist knots (Haney et al., 2020).

The objective of this study is to determine if the skins of hagfish are morphologically or functionally different across species. Using a series of uniaxial and synchronized equibiaxial testing, gross dissection, and histological approaches, we gathered data sets from the skins of four hagfish species spanning the Eptatretinae and Myxininae to determine if the characteristics previously recorded in *E. stoutii* skins (Clark et al., 2016) are conserved in the skins of other species. For broader comparative purposes, we also gathered similar data from the skins of an outgroup, the American eel *Anguilla rostrata* (Lesueur, 1817).

2. Materials and Methods

2.1. Specimens

Data presented in this study were gathered from the skins of two hagfish species from the subfamily Myxininae: the Atlantic hagfish *Myxine glutinosa* Linnaeus, 1758 and the Eastern Pacific Myxinine *Myxine hubbsi* Wisner & McMillan, 1995, and two hagfish species from the subfamily Eptatretinae: the Gulf hagfish *Eptatretus springeri* (Bigelow & Schroeder, 1952) and the Pacific hagfish *Eptatretus stoutii* (Lockington, 1878). For comparison, additional data sets were gathered from the skins of the American eel *Anguilla rostrata* (Lesueur, 1817), a local and readily available species of elongate teleost. *A. rostrata* is a commonly-studied representative of the eel family, Anguillidae, that possesses taut-skin and does not perform knotting, however, rotational feeding has been observed in some specimens (Helfman and Clark, 1986). Skin samples subjected to uniaxial tensile tests were collected from five individuals of *M. glutinosa* (total length, TL = 51.8 – 58.4 cm), eight individuals of *M. hubbsi* (TL = 53.3 – 67.3 cm), eight individuals of *E. stoutii* (TL = 45.2 – 54.0 cm), three individuals of *E. springeri* (TL = 49.2 – 56.6 cm), and five individuals of *A. rostrata* (TL = 39.4 – 57.8 cm). From this collection of animals, we subjected skin samples from four *A. rostrata*, five *E. stoutii,* and five *M. glutinosa* to biaxial tensile tests.

Among the four species of hagfish studied here, *E. stoutii* and *M. glutinosa* are more accessible to North American researchers, and because of this, we were able to test fresh samples of skin from these species. Live specimens of *M. glutinosa* were shipped from the NOAA NMFS (Gloucester, ME) to our research laboratory at the College of Charleston (Charleston, SC). Live specimens of *E. stoutii* were shipped to our lab from the Washington Department of Fish and Wildlife and the Olympic Seafood Company (Olympia, WA). At the lab, the animals were housed in custom aquaria with recirculating artificial saltwater maintained at approximately 10 °C and 35 ppt. (Gustafson, 1935). The aquaria were shaded and securely covered to block ambient light and to prevent escape. Prior to preparing skin samples for material testing, a specimen of *E. stoutii* or *M. glutinosa* was either euthanized with an overdose of tricaine methanesulfonate or died incidentally. The care and use of living specimens of *M. glutinosa* and *E. stoutii* were conducted under the approval of the IACUC (Protocol 2015-002) from the College of Charleston. Live specimens of *E. springeri* were housed at Valdosta State University, and the care and handling of this species was approved by the IACUC at VSU (VSU AUP-00070-2017).

We gathered data sets from frozen specimens of the lesser known and less accessible species: *E. springeri* and *M. hubbsi*. Specimens of *E. springeri* were shipped to our lab from the Florida State University Coastal and Marine Laboratory (St. Teresa, FL) and specimens of *M. hubbsi* were shipped from the California Fish and Game Commission (San Pedro, CA). At the lab, these specimens were kept frozen at approximately −30 °C until experimentation. Specimens of *E. springeri* and *M. hubbsi* were euthanized with an overdose of tricaine methanesulfonate (MS-222) prior to freezing at approximately −30 °C until experimentation. Euthanized specimens of *A. rostrata*, previously surveyed by the South Carolina Department of Natural Resources (Charleston, SC), were subsequently sent to our lab and were also kept frozen prior to the experiments.

2.2. Uniaxial Tensile Testing

Skins used for uniaxial testing were dissected from the left and right sides of each animal at approximately 50% TL (Fig. 2A). The skin dissected from each animal was then cut into eight testing samples; four were shaped as dumbbells and four were shaped as rectangles. The shape of the dumbbell has a definitive location where the cross-sectional area is smallest, and when placed in tension, is where tensile stress contours are concentrated and mechanical failure must occur. Material properties relating to failure were determined from stress-strain data on the skin dumbbells (see below). We used the methods described in Clark et al. (2016) for preparing and testing two rectangular skin samples and two dumbbell skin samples for each direction of applied strain. The long axis of each skin sample was oriented along either the animal's longitudinal or circumferential axis (Fig. 2A). Individual rectangular samples were typically 4.0 mm wide and 12.0 mm long, whereas the dumbbells were 1.5 mm wide (at the narrowest part of the sample) and 12.0 mm long (following Clark et al., 2016). Hagfish skin samples were kept moist within folded lintless paper wipes dipped in salt water (10 – 12 °C, 34 – 36 ppt) and briefly blotted before testing. This approach, using salt water diluted to 12 – 13 ppt, was also used for keeping samples of *A. rostrata* skins moist.

Uniaxial tensile tests were performed with an IMADA EMX-275 motorized testing stand rigged with a 500N-capacity IMADA ZP-110 force gauge and a Mitutoyo Digimatic height gauge (Fig. 2B). Each skin sample was clamped between a stationary grip and actuating grip, then stretched at a rate of 25.0 mm min^{-1} until the sample broke. During the test, the applied force and distance data sets were acquired with IMADA SW2.X software. The gripped ends of the skin samples were secured within small folded sections of 80-grit sandpaper to prevent slippage. Before initiating each test, we measured the sample's width, thickness, and initial length (or grip separation) with digital calipers (Fig. 2B, C). Measured force-length data were subsequently converted to stress-strain data, from which we calculated material properties. The skin sample's cross-sectional area (CSA) orthogonal to the applied tensile force (F) equaled the product of the width and thickness. Engineering stress (σ) was obtained by using the equation $\sigma = F/CSA$, and engineering strain (ε) was calculated as $\varepsilon = \Delta L/L_0$, where ΔL equals the change in the test sample's length during the tensile test, and L_0 equals the sample's initial length prior to pulling. Using the stress-strain recordings from dumbbell-shaped skin samples, we measured peak stress (or strength), peak strain (or extensibility), and strain energy storage (sometimes called 'toughness'). The strain energy stored by a skin sample equals the area under the stress-strain curve, which was

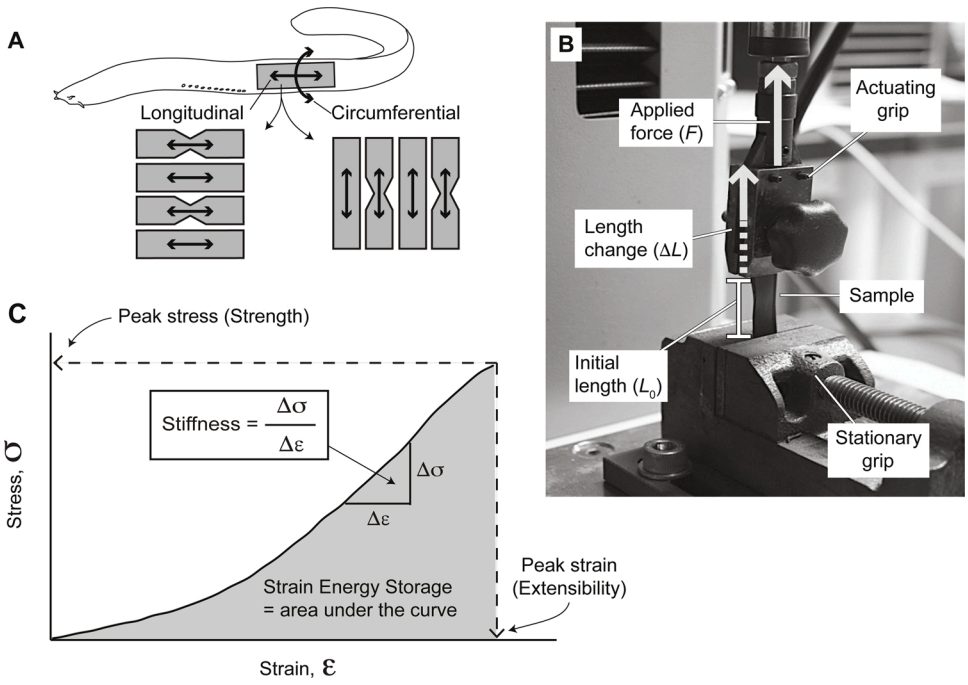

Fig. 2. Methods for conducting quasi-static uniaxial tensile tests to failure. (A) Approaches for dissecting skin from the animals and the fabrication of test samples for tensile tests. (B) Photograph of the region of the uniaxial testing rig where test samples were clamped and stretched. Included are the parameters for measuring sample dimensions. (C) Representative stress-strain curve illustrating the methods used for determining material properties from destructive uniaxial testing procedures.

calculated with trapezoidal Riemann sums. Elastic modulus or "stiffness" (E), which was calculated as $E = \Delta\sigma/\Delta\varepsilon$, was determined from the linear elastic regions of the stress-strain curves from rectangular-shaped skin samples (Fig. 2C).

We used destructive approaches for measuring material properties like strength and extensibility because 1) these peak data are relevant to the extremely large deformations achieved by hagfish bodies during knotting and injurious attacks, 2) these data describe some of the performance capacities of hagfish skins, 3) these procedures are simple, repeatable, and informative, and 4) hagfish skins are poorly studied and future investigations deserve analyses using nondestructive approaches.

2.3. Biaxial Tensile Testing

We performed a series of planar equibiaxial tensile tests to failure by using a custom testing rig equipped with a pair of orthogonally oriented 250N-capacity load cells (ADMET Inc.). This two-axis system included two fast-acting servo drive motors that could achieve maximum speeds

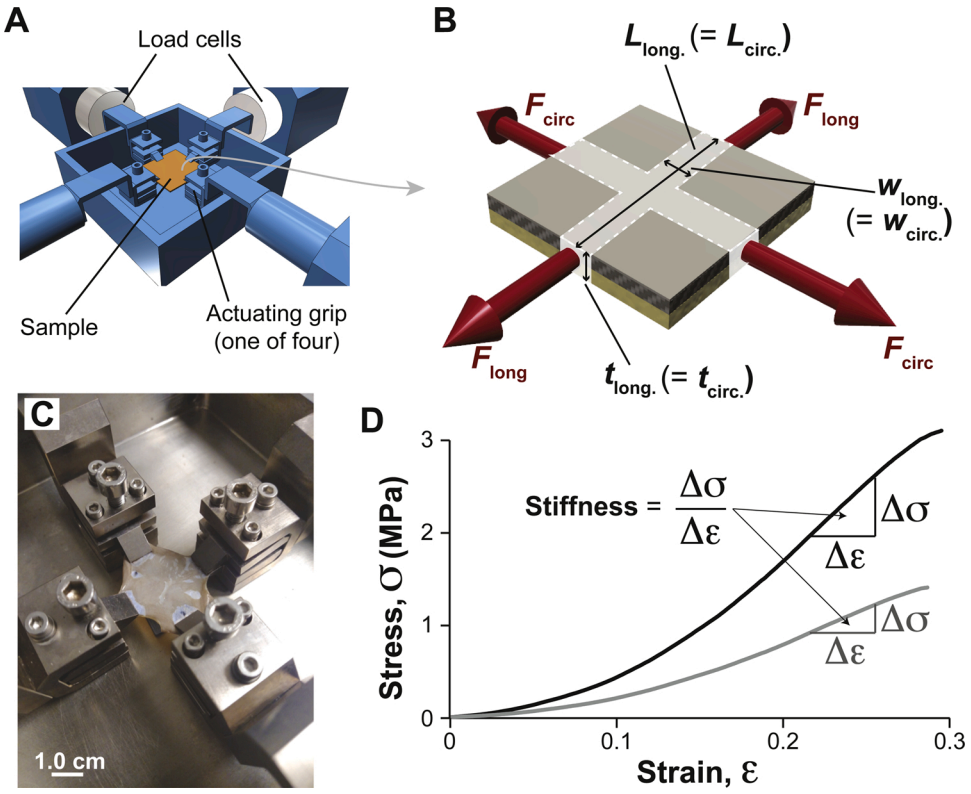

Fig. 3. Methods for synchronized planar equibiaxial tensile testing. (A) Illustration of the planar biaxial testing system. (B) Schematic of a skin sample under biaxial tension. The length and width of each sample were measured between the grips once the sample was clamped, not the original dimensions of the sample itself. (C) Photograph of a sample of hagfish skin clamped in the biaxial testing rig during mechanical failure. (D) Representative stress-strain curves acquired from a biaxial test performed on a skin sample from Pacific hagfish *Eptatretus stoutii*, including the approaches used for measuring biaxial stiffness.

of 250 mm·min^{-1} along both axes. The machine's crossheads used twin ball-screw actuators to move symmetrically about the center lines of the test space and each axis was programmed for coordinated motion in MTESTQuattro®. From each specimen of *A. rostrata*, *E. stoutii,* and *M. glutinosa*, we fabricated three 2.54 cm^2 square-shaped skin samples for biaxial testing approaches (Fig. 3). Skin samples were gathered from the flanks of each animal at approximately 50% *TL* and approximately 5 – 8 mm of the samples' edges were clamped within four 10 mm wide grips. To prevent the samples from slipping during testing, small folded sections of 80-grit sandpaper were clamped between the outer surface of the skin sample and the inner surface of each grip.

Initial length of each sample at each axis, or grip separation, was measured with digital calipers before testing was initiated. Skin samples were simultaneously strained in longitudinal and circumferential axes at equal rates of 25.0 mm min^{-1} until failure and the force-displacement data were sampled at 100 Hz. During the course of each test, positions were measured as the distances between grips in both axes with a position resolution of 0.13 μm. *CSA* along each axis equaled the product of the grip width (1.0 cm) and the sample's thickness. Using these data, we converted the force-displacement curves to stress-strain curves for determining the biaxial stiffness (Fig. 3D).

2.4. Comparative Morphology

From each species of hagfish, we collected six rectangular samples of skin for morphological analysis: three samples from the head region (20 – 25% *TL*) and three from the tail region (75 – 80% *TL*). Sliced edges of these samples were positioned under a dissection microscope and digitally photographed. We used ImageJ (Rasband, 1997) to measure the dermal and hypodermal thicknesses from these photographs. The total thickness of the skin equals the sum of the dermal thickness and hypodermal thicknesses. All measurements were performed on fresh samples of skin devoid of preservation artifacts (e.g. shrinkage due to fixation). We also performed histological analyses of skin samples in our research laboratory at VSU. To ensure that the skin samples used for histology were harvested in similar states of low or no tension, specimens of *E. stoutii*, *M. glutinosa,* and *E. springeri* were euthanized in similarly relaxed states. Representative skin samples were pinned onto pink extruded polystyrene insulation foam boards prior to fixation in 10%-neutral buffered formalin. Pinning our skin samples in this manner preserved their original length, width, and fiber angle during the fixation process. Samples were subsequently dehydrated with ethanol, embedded in paraffin, and sectioned at 8 – 12 μm thick. Both transverse and grazing longitudinal sections were cut and stained with a modified Milligan's trichrome (Kier, 1992). Sections were then visualized microscopically using phase contrast illumination for maximal contrast enhancement of muscle and connective tissue fiber orientations. The Milligan's trichrome protocol stains muscle tissue magenta, collagen blue, erythrocytes orange, and nuclei red. Histological sections were then digitized and the skin morphology was described. Transverse sections were used to characterize the strata and components of the skin. Grazing sections were used to measure tissue fiber angles relative to the long axis of the body.

2.5. Data Analysis

Data sets for each material property (stiffness, strength, extensibility, and toughness) were organized by species (*M. hubbsi*, *M. glutinosa*, *E. stoutii*, *E. springeri*, and *A. rostrata*) and body axis (direction of tension applied during testing). From each animal, we calculated the mean data from two skin samples specific to a direction and species. From these individual means, we calculated grand means for species and body axis, which were subsequently analyzed. Normality of these material properties data was tested using Shapiro-Wilk tests and all data sets met normality following log-transformations. All of the log-transformed data were statistically tested in JMP Pro 14 while raw data sets were graphed. Transformed uniaxial testing data were compared using a factorial ANOVA with all species, direction of applied tension, and interactions between species and direction as main effects. *Post hoc* tests included Tukey multiple comparison tests for comparing mean data across species, followed by t-tests with Bonferroni corrections for comparing mean data between longitudinal and hoop axes within each species and for comparing mean data between hagfish species belonging to the same genus (*Myxine* or *Eptatretus*). To compare biaxial stiffness, we used a 3 × 2 factorial ANOVA with species (*A. rostrata*, *E. stoutii*, and *M. glutinosa*), direction, and interactions as effects, followed by a Tukey multiple comparison test to compare mean data between *A. rostrata*, *E. stoutii,* and *M. glutinosa* followed by t-tests with Bonferroni corrections for comparing mean data between axes. Skin thickness data gathered from the hagfish species were compared with a 4 × 2 factorial ANOVA with species, location, and interactions as effects. *Post hoc* Tukey multiple comparison tests were then used for comparing mean thicknesses across species followed by t-tests with Bonferroni corrections for comparing mean data between species belonging to the same genus. Mean data sets between the head and tail regions of the hagfishes were also compared by using t-tests and Bonferroni corrections. We used $P < 0.05$ as the criterion for significance in the ANOVAs and $P < 0.025$ for t-tests.

3. Results

3.1. Material Properties

Using both uniaxial and biaxial tensile tests, we found differences in the material properties of the skins from the four species of hagfish examined, and collectively, the material properties of all types of the hagfish skins differed from those of American eel skins (Figs. 4 and 5; Table 1). Significant differences in stiffness ($F_{4, 48} = 7.271$, $p = 0.0001$) and extensibility ($F_{4, 48} = 2.999$, $p = 0.027$) depended on the direction of applied strain and the species (Table 1). The skins from *Eptatretus* were anisotropic, being approximately twice as stiff in the longitudinal axis than in the circumferential axis ($p = 0.001$ in *E. springeri* and $p = 0.006$ in *E. stoutii* (Table 1; Fig. 4A). Strength ($p = 0.020$) and extensibility ($p = 0.004$) of *E. stoutii* skins were also significantly different between longitudinal axis than in the circumferential axis (Table 1; Fig. 4B, C). In contrast to *Eptatretus*, the skins from *Myxine* were isotropic with similar stiffness along both directions of applied tension ($p = 0.096$ in *M. hubbsi* and $p = 0.738$ in *M. glutinosa*; Table 1; Fig. 4A). In contrast to hagfish skins, *A. rostrata* skins were twice as stiff in the circumferential axis than in the longitudinal axis ($p = 0.008$; Table 1; Fig. 4A).

American eels possessed the stiffest (mean stiffness ± s.e.m. up to 233 ± 28.8 MPa) and strongest (up to 62.4 ± 9.59 MPa) skins of all species, and along with *E. stoutii* skins, were the toughest (up to 4.83 ± 0.67 MJ m^{-3}; Table 1; Fig. 4C). Conversely, skins from *E. springeri* were the least stiff (5.89 ± 0.71 MPa), least strong (4.46 ± 0.84 MPa), and absorbed the least amount of strain energy (0.82 ± 0.26 MJ m^{-3}) prior to failure (Table 1; Fig. 4). Skins from both species of *Eptatretus* were more extensible than the skins from *M. glutinosa* and *M. hubbsi*. Samples of *E. springeri* and *E. stoutii* skins stretched to 47-48% of their original lengths prior to mechanical failure (Table 1; Fig. 4C).

Significant differences in biaxial stiffness ($F_{2, 22} = 6.503$, $p = 0.006$) depended on the direction of applied strain and the species (Table 2; Fig. 5). Mean stiffness of Atlantic and Pacific hagfish skin samples subjected to equibiaxial tension was smaller in magnitude than when subjected to uniaxial tension. In contrast, biaxially-strained American eel skin samples were stiffer than uniaxially-strained skins and were three times stiffer than the skins of both *E. stoutii* and *M. glutinosa* (Fig. 5). Samples of *E. stoutii* and *A. rostrata* skins exhibited the anisotropy previously observed in uniaxially strained samples, with *E. stoutii* skins being stiffer in the longitudinal axis and *A. rostrata* skins being stiffer in the circumferential axis (Table 2; Fig. 5). As in the uniaxial tests, *M. glutinosa* skins were isotropic under equibiaxial tension.

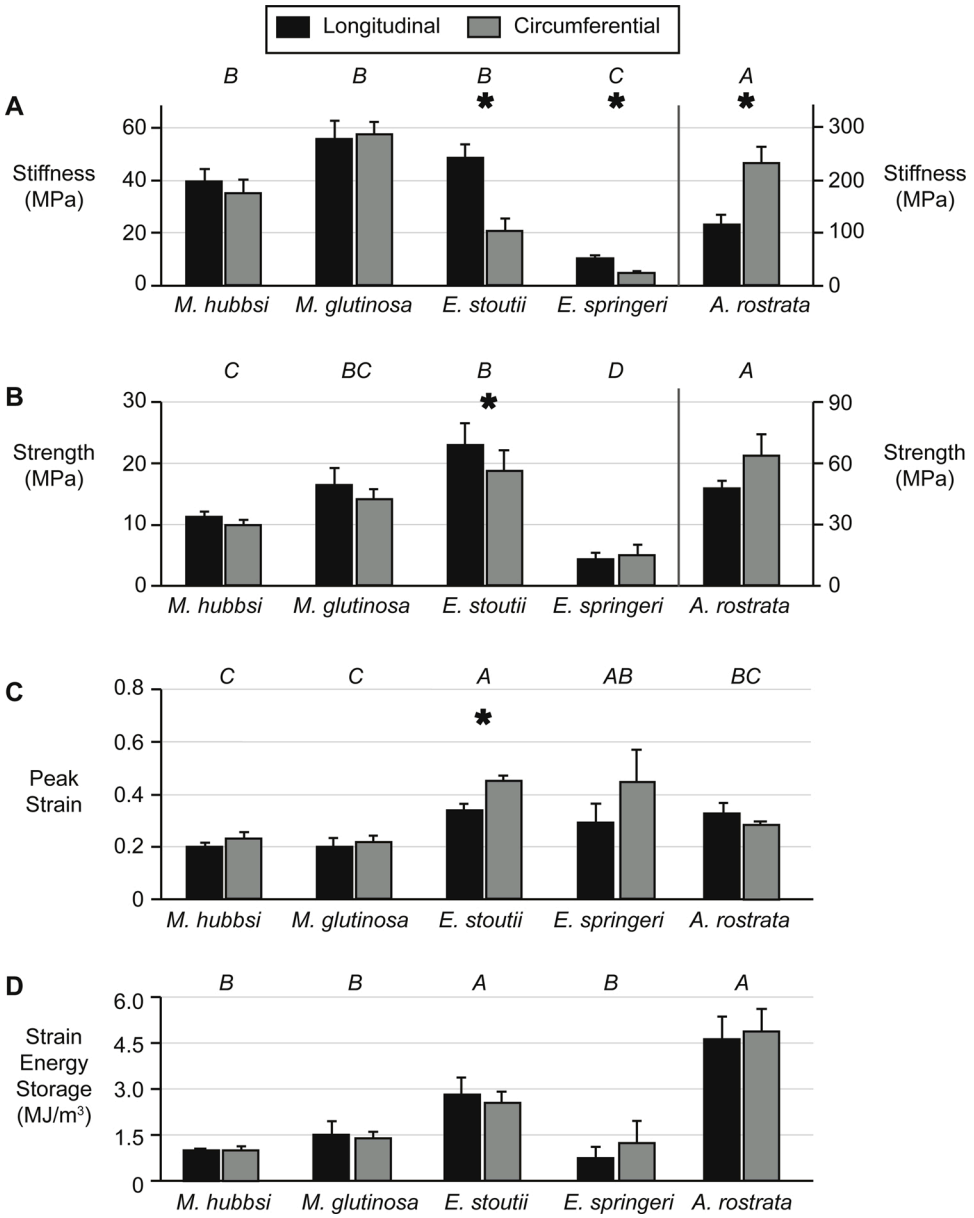

Fig. 4. Material properties from uniaxial testing data. Mean data ± s.e.m. for uniaxial tensile tests along both longitudinal and circumferential axes of all four species of hagfish and the eel *A. rostrata*. Material properties represented are (A) stiffness (B) strength (a.k.a. peak stress) (C) peak strain (a.k.a. extensibility) and (D) strain energy storage (a.k.a. toughness). Species data not sharing the same capital letter are significantly different. Asterisks represent significant differences between longitudinal and circumferential axes within a species.

3.2. Comparative Morphology

Fresh samples of hagfish skins under a dissection microscope reveal the absence of scales and further investigations of histological sections viewed under a light microscope show the skin is composed of multiple strata. The skins of all hagfish species examined possess three strata: a thin epidermis superficial to a conspicuously thick dermis (*stratum compactum*) comprising several densely-packed layers of collagen fibrils, which in turn is superficial to a comparably thick hypodermis (*stratum laxum*) mainly composed of adipose tissue (Fig. 6). The superficial and deep borders of the dermis layer contain epidermal basal lamina and dermal endothelium, respectively. These findings were also reported by Welsch et al. (1998) and Weinrauch et al. (2016).

Significant differences in total skin thickness ($F_{3, 30} = 48.706$, $p < 0.0001$) depended on the location on the body and the species of the hagfish (Table 3). Differences in skin thickness between cranial and caudal regions were only noted in specimens of *M. hubbsi* and *E. stoutii* (Table 3). *E. springeri* possessed the thickest of skins and their dermises (up to 0.515 ± 0.022 mm) were almost three times as thick as the dermal layers of *E. stoutii*, *M. glutinosa*, and *M. hubbsi* skins, which ranged from approximately 0.150 mm to 0.200 mm (Table 3; Fig. 6).

Histological sections of the dermis from both species of *Eptatretus* possessed fibers that stained either magenta or blue. The samples of *Myxine* skin were very different: there were no components that stained magenta, and only fibers that stained blue (Fig. 7). Grazing parasagittal sections show that the fibers within in the dermis of *E. stoutii* skins were wavy, in contrast to the straighter fibers in *M. glutinosa* and *M. hubbsi* (Fig. 7B–E). Despite these differences, the skins of *E. stoutii*, *M. glutinosa*, and *M. hubbsi* possessed similar fiber angles that ranged from 44° to 46°. However, we were not able to produce sections of *E. springeri* skins that clearly showed fiber angles within the dermis, which precluded us from reporting fiber angles in this species (Fig. 7D).

4. Discussion

The impetus of the current study was to expand previous research (Clark et al., 2016) that investigated the material properties from one species of *Eptatretus* in order to determine if the skins are functionally and morphologically different across hagfish taxa. Across four species of hagfishes representing the two dominant lineages of the Myxinindae, we

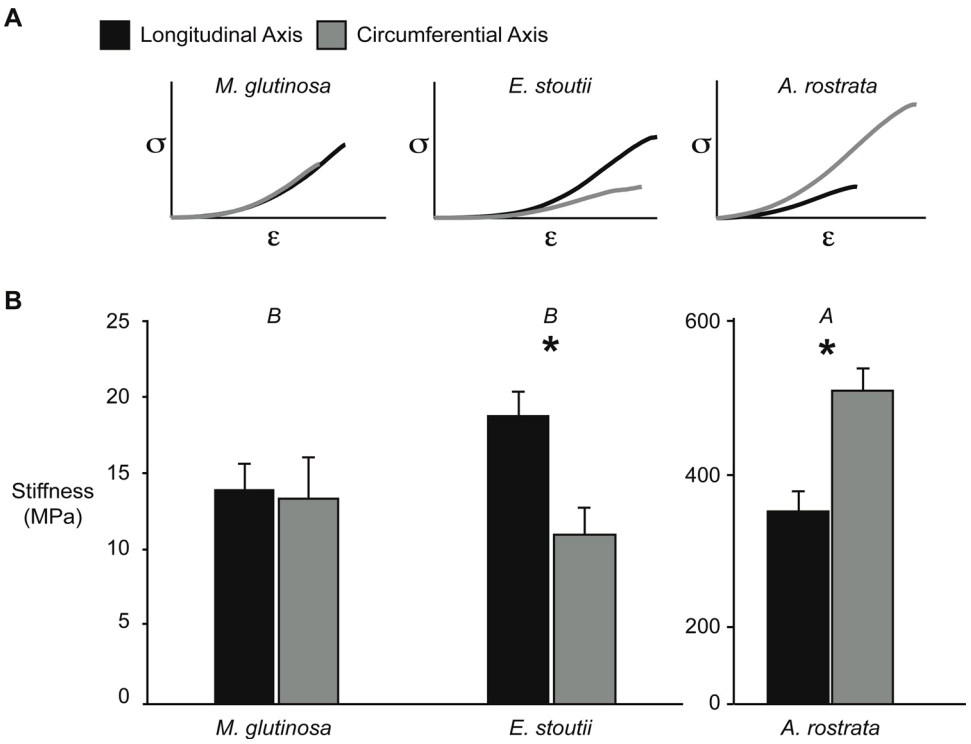

Fig. 5. Material properties from biaxial testing data. (A) Representative stress-strain curves from planar equibiaxial tensile tests to failure from the skins of *M. glutinosa, E. stoutii,* and *A. rostrata*. (B) Biaxial stiffness (mean ± s.e.m.) in longitudinal and circumferential axes. Species data not sharing the same capital letter posted above the bar graphs are significantly different. Asterisks represent significant differences between body axes within a species.

found noteworthy interspecific differences in the morphology and material properties of the skins. Eptatretines possess anisotropic skins with dermises containing a lattice of collagen fibrils interwoven with fibers that stain like muscle tissue. These characteristics contrast those of the skins from Myxinines, which are isotropic and have dermises containing fibrous tissues that only stain like collagen. There are parallels between this phylogenetic pattern, the diverse forms and functions of the skin, and the diverse body knotting behaviors observed across these species.

4.1. Diversity in the Material Properties of Hagfish Skins

In the current study, we show that the skins of two representatives of Myxinines and two representatives of Eptatretines have genus-specific functions and morphologies. Using biaxial and uniaxial tensile tests to failure, we find that the skins of *Eptatretus* are nearly twice as stiff in the longitudinal axis than in the circumferential axis, which contrasts the isotropic skins of *Myxine* (Figs. 4 and 5; Tables 1 and 2). *Eptatretus* skins were more than twice as extensible as *Myxine* skins (Fig. 4C; Table 1), and in some skin samples from *E. stoutii*, we recorded circumferentially directed peak strains as large as 0.58. The anisotropy observed in the *E. stoutii* skins from the present study corroborates results from previous tensile tests (Clark et al., 2016) and some results from inflation tests (Boggett et al., 2017). Furthermore, the material properties data gathered from fresh samples of *E. stoutii* skins in this study are surprisingly similar to data previously collected from thawed samples (Clark et al., 2016). Multiple studies have shown that the formation of ice crystals during freezing can damage tissues and reduce its strength and stiffness (e.g. Micozzi, 1986). Freezing has also been shown to affect the material properties of rabbit skins (Billingham and Medawar, 1951), harbor seal skins (Grear et al., 2018), human skins and porcine skins (Ranamukhaarachchi et al., 2016), however, we know relatively little about the effects of freezing and thawing on the biomechanics of fish skins. Nonetheless, it is worth noting that freezing imposes the least structural and mechanical changes of any storage methods (Ranamukhaarachchi et al., 2016).

The material properties of the skin can also differ among hagfish species of the same genus. Within *Eptatretus*, we found large differences in the magnitudes of material properties (Fig. 4; Table 1), with the skins of *E. stoutii* being four times stiffer in the circumferential axis and three times stiffer in the longitudinal axis than *E. springeri* skins (Fig. 4A). The variation material properties across the hagfish species in the current study could be related to differences in their knotting kinematics; increased compliance and extensibility in *Eptatretus* skins might permit more body core deformations which aid in the formation of a greater diversity of knot styles relative to *Myxine* (Haney et al., 2020).

Fresh samples of skins from *A. rostrata*, *E. stoutii*, and *M. glutinosa* exhibited the same mechanical responses to equibiaxial tension as they did to uniaxial tension; both testing methods yielded similar ratios of mean longitudinal-axis stiffness (E_L) to mean circumferential-axis stiffness (E_C). The E_L:E_C ratio for an isotropic material is 1.0, which is closely matched by the E_L:E_C ratio for *M. glutinosa* skin samples from biaxial tests (1.01) and uniaxial tests (0.97). Alternatively, anisotropic skins have E_L:E_C ratios considerably greater than or less than 1.0 (Fig. 8A). In *E. stoutii*, the E_L:E_C ratio of the skin samples were 1.72 in biaxial tests and 1.70 in uniaxial tests, and in *A. rostrata* skins, the ratios equaled 0.65 in biaxial tests and 0.49 in uniaxial tests (Fig. 8A). Results from equibiaxial tensile tests on the skins of the haddock *Melanogrammus aeglefinus* (Waldman and Lee, 2005) also show that the skins are significantly stiffer circumferentially than longitudinally. More broadly, the tensile stiffness of skins from other species of teleosts (e.g. Hebrank and Hebrank, 1986) and cartilaginous fishes (e.g. Naresh et al., 1997) are also substantially higher in the circumferential direction.

In earlier studies, pressurized closed-ended cylinders were readily considered models for undulating elongate fishes (Hebrank, 1980) and the anisotropy in the fish skins were partially explained by Laplace's law. This law states that the pressurization of incompressible fluid within a cylinder's cavity exerts twice the amount of tensile stress along the circumferential axis of the cylinder's wall, which is assumed to be inextensible and isotropic. Therefore, a pressurized cylinder wall should be stiffer in tension along its circumferential axis (Vogel, 2013).

Table 1
Differences in the material properties obtained from uniaxial tensile tests associated with the effects of all fish species and the direction of applied tension (top table). *Post hoc* comparisons of material properties between species and between direction of applied tension are included below. *P*-values < 0.05 are in bold text.

All fishes	Stiffness		Strength		Extensibility		Toughness	
	F	*p*	F	*p*	F	*p*	F	*p*
Species	79.679	**< 0.0001**	37.138	**< 0.0001**	17.104	**< 0.0001**	18.643	**< 0.0001**
Direction	2.308	0.135	0.022	0.882	2.912	0.094	0.331	0.568
Sp x Dir	7.271	**0.0001**	0.753	0.753	2.999	**0.027**	0.177	0.949

Stiffness:

Group Comparison		Difference	SE	Lower CL	Upper CL	*P*-value
A. rostrata	*E. springeri*	2.91	0.19	2.36	3.45	**< 0.0001**
M. glutinosa	*E. springeri*	1.87	0.19	1.34	2.41	**< 0.0001**
M. hubbsi	*E. springeri*	1.49	0.19	0.95	2.02	**< 0.0001**
A. rostrata	*E. stoutii*	1.47	0.19	0.93	2.01	**< 0.0001**
E. stoutii	*E. springeri*	1.44	0.19	0.90	1.99	**< 0.0001**
A. rostrata	*M. hubbsi*	1.43	0.19	0.89	1.96	**< 0.0001**
A. rostrata	*M. glutinosa*	1.04	0.19	0.50	1.58	**< 0.0001**
M. glutinosa	*E. stoutii*	0.43	0.19	−0.10	0.97	0.1666
M. glutinosa	*M. hubbsi*	0.39	0.19	−0.15	0.93	0.2589
M. hubbsi	*E. stoutii*	0.06	0.19	−0.49	0.58	0.9992

Strength:

Group Comparison		Difference	SE	Lower CL	Upper CL	*P*-value
A. rostrata	*E. springeri*	2.45	0.17	1.97	2.94	**< 0.0001**
A. rostrata	*M. hubbsi*	1.63	0.17	1.14	2.12	**< 0.0001**
E. stoutii	*E. springeri*	1.35	0.17	0.86	1.84	**< 0.0001**
A. rostrata	*M. glutinosa*	1.27	0.17	0.78	1.76	**< 0.0001**
M. glutinosa	*E. springeri*	1.18	0.17	0.69	1.67	**< 0.0001**
A. rostrata	*E. stoutii*	1.11	0.17	0.62	1.60	**< 0.0001**
M. hubbsi	*E. springeri*	0.82	0.17	0.33	1.31	**0.0002**
E. stoutii	*M. hubbsi*	0.53	0.17	0.04	1.01	**0.029**
M. glutinosa	*M. hubbsi*	0.36	0.17	−0.13	0.85	0.243
E. stoutii	*M. glutinosa*	0.17	0.17	−0.32	0.66	0.868

Extensibility:

Group Comparison		Difference	SE	Lower CL	Upper CL	*P*-value
E. stoutii	*M. glutinosa*	0.72	0.13	0.36	1.08	**< 0.0001**
E. stoutii	*M. hubbsi*	0.65	0.13	0.29	1.01	**< 0.0001**
E. springeri	*M. glutinosa*	0.45	0.13	0.099	0.80	**0.0085**
E. stoutii	*A. rostrata*	0.41	0.13	0.05	0.77	**0.0194**
E. springeri	*M. hubbsi*	0.38	0.13	0.02	0.73	**0.0368**
A. rostrata	*M. glutinosa*	0.31	0.13	−0.05	0.67	0.1219
E. stoutii	*E. springeri*	0.27	0.13	−0.09	0.63	0.2205
A. rostrata	*M. hubbsi*	0.24	0.13	−0.12	0.60	0.3352
E. springeri	*A. rostrata*	0.14	0.13	−0.22	0.50	0.8194
M. hubbsi	*M. glutinosa*	0.07	0.13	−0.29	0.43	0.9812

Toughness:

Group Comparison		Difference	SE	Lower CL	Upper CL	*P*-value
A. rostrata	*E. springeri*	1.72	0.21	1.11	2.33	**< 0.0001**
A. rostrata	*M. hubbsi*	1.59	0.21	0.99	2.20	**< 0.0001**
E. stoutii	*E. springeri*	1.26	0.21	0.65	1.87	**< 0.0001**
A. rostrata	*M. glutinosa*	1.23	0.21	0.62	1.83	**< 0.0001**
E. stoutii	*M. hubbsi*	1.13	0.21	0.52	1.74	**< 0.0001**
E. stoutii	*M. glutinosa*	0.76	0.21	0.15	1.37	**0.0078**
M. glutinosa	*E. springeri*	0.50	0.21	−0.11	1.12	0.1576
A. rostrata	*E. stoutii*	0.47	0.21	−0.14	1.07	0.2090
M. glutinosa	*M. hubbsi*	0.37	0.21	−0.24	0.98	0.4291
M. hubbsi	*E. springeri*	0.13	0.21	−0.48	0.74	0.9753

	Myxine hubbsi		
Material Property	Longitudinal	Circumferential	*P*-value
Stiffness (MPa)	40.8 ± 7.47	40.1 ± 6.45	0.096
Strength (MPa)	10.9 ± 1.21	10.1 ± 1.36	0.623
Extensibility	0.21 ± 0.02	0.22 ± 0.02	1.000
Toughness (MJm^{-3})	0.97 ± 0.08	0.90 ± 0.11	0.556

	Myxine glutinosa		
Material Property	Longitudinal	Circumferential	*P*-value
Stiffness (MPa)	55.6 ± 6.69	59.0 ± 4.50	0.738
Strength (MPa)	16.4 ± 2.71	14.1 ± 1.61	0.573
Extensibility	0.20 ± 0.03	0.22 ± 0.02	1.000
Toughness (MJm^{-3})	1.53 ± 0.41	1.39 ± 0.21	0.992

	Eptatretus stoutii		
Material Property	Longitudinal	Circumferential	*P*-value
Stiffness (MPa)	52.3 ± 6.13	26.5 ± 2.87	**0.006**
Strength (MPa)	24.5 ± 3.16	13.4 ± 2.56	**0.020**
Extensibility	0.32 ± 0.03	0.48 ± 0.03	**0.004**
Toughness (MJm^{-3})	3.29 ± 0.59	2.70 ± 0.37	0.479
	Eptatretus springeri		
Material Property	Longitudinal	Circumferential	*P*-value
Stiffness (MPa)	13.0 ± 1.25	5.89 ± 0.71	**0.001**
Strength (MPa)	4.46 ± 0.84	5.62 ± 1.53	0.651
Extensibility	0.31 ± 0.05	0.47 ± 0.09	1.000
Toughness (MJm^{-3})	0.82 ± 0.26	1.37 ± 0.53	0.489
	Anguilla rostrate		
Material Property	Longitudinal	Circumferential	*P*-value
Stiffness (MPa)	116 ± 17.4	233 ± 28.8	**0.008**
Strength (MPa)	47.0 ± 3.32	62.4 ± 9.59	0.268
Extensibility	0.32 ± 0.04	0.22 ± 0.01	0.053
Toughness (MJm^{-3})	4.58 ± 0.67	4.83 ± 0.67	0.779

Post hoc tests:
Multiple comparisons of log-transformed material properties data from all species using Tukey-Kramer Honest Significance Tests. *P*-values < 0.05 are in bold text.
T-test results comparing material properties between longitudinal and circumferential axes per species. Data are means ± s.e.m. *P*-values < 0.025 are in bold text.

Table 2
Differences in biaxial stiffness associated with the effects of all fish species and direction of applied tension. *Post hoc* comparisons of biaxial stiffness between species and between direction of applied tension are included below. *P*-values < 0.05 are in bold text.

	Biaxial Stiffness	
All fishes	F	*p*
Species	67.477	**< 0.0001**
Direction	0.806	0.135
Sp x Dir	6.503	**0.006**

Group Comparison		Difference	SE	Lower CL	Upper CL	*P*-value
A. rostrata	*M. glutinosa*	387	29.6	313	460	**< 0.0001**
A. rostrata	*E. stoutii*	386	29.6	313	460	**< 0.0001**
E. stoutii	*M. glutinosa*	0.21	27.9	−69.2	69.7	1.0000

Species	Longitudinal	Circumferential	*P*-value
E. stoutii	18.9 ± 1.63 MPa	11.2 ± 1.72 MPa	**0.0172**
M. glutinosa	14.0 ± 1.81 MPa	13.5 ± 2.63 MPa	0.7308
A. rostrata	305 ± 30.1 MPa	496 ± 32.5 MPa	**0.0068**

Post hoc tests:
Multiple comparisons of log-transformed biaxial testing data from American eels, Atlantic hagfish, and Pacific hagfish using Tukey-Kramer Honest Significance Tests.
Comparing biaxial stiffness between longitudinal and circumferential axes per species using T-tests and Bonferroni corrections. Data are means ± s.e.m. *P*-values < 0.025 are in bold text.

Anisotropic skins with more resistance to circumferentially-directed stresses and strains appear to be commonplace among teleosts and sharks. However, recordings of intramuscular pressures generated in teleost fishes (Horton et al., 2004) and cartilaginous fishes (Martinez et al., 2003) did not reveal the elevation of intramuscular pressure with increasing swimming speeds reported by Wainwright et al. (1978). These discrepancies ultimately suggest that whole bodies of many fishes are poorly represented by pressurized cylindrical vessels (Summers and Long, 2006). Moreover, the morphology of elongate fishes typically violates two important assumptions of Laplace's law: 1) their bodies are bilaterally-compressed with elliptical cross-sections, in contrast to the circular cross-sections of cylinders, and 2) their skins are anisotropic and extensible. Given their extensibilities and the tapering (bilateral compression) of the caudal ~30% of their *TL*, hagfishes also violate these assumptions.

A more probable explanation for the anisotropy observed in most fish skins is the orientation of tension-resistant fibers comprising the dermis (Clark and Cowey, 1958; Hebrank, 1980). The dermal regions of fish skins possess cross-helical arrangements of collagen fibers that intersect with the long axis of the fish at variable fiber angles that are particularly useful in preventing the body from kinking while bending (Motta, 1977). Fiber angles govern the deformational characteristics of pressurized bodies and their body coverings (Clark and Cowey, 1958; Vogel, 2013). For example, a cylindrically-shaped organism that is pressurized cannot change in diameter or length if its fiber angles are equal to 54.7° relative to the long axis (Clark and Cowey, 1958). If this organism's skin is not under tension (i.e. the body is less pressurized or the skin does not contain a maximal volume), then muscle actions that result in increases in body length will reduce the cross-helical fiber angle. Similarly, increases in body diameter will result in an angle that is greater than 54.7°. At some point, body deformations reconfigure fiber angles to become longitudinal or circumferential enough that they resist further deformations, and internal pressure begins to increase. The skins of most teleosts (Hebrank and Hebrank, 1986; Kenaley et al., 2018) and cartilaginous fishes (Motta, 1977; Naresh et al., 1997) possess fiber angles ranging from 50° to 70°, with some approaching 54.7° (Szewciw and Barthelat, 2017). This phenomenon was also a motivating factor in developing the whole-body exotendon hypothesis introduced by Wainwright et al. (1978), however, fiber angles nearing 54.7° also occur in fish skins that do not function like exotendons (Hebrank and Hebrank, 1986). With fiber angles ranging from 50° to 70°, and thus having preferred orientations towards the circumferential axis, it is reasonable to expect the skins of most cartilaginous and bony fishes to be more resistant to tensile strains applied along the circumferential axis than to strains applied in the longitudinal axis. For example, fiber angles ranging from approximately 58° to 60° have been identified in the skins of *A. rostrata* (Danos et al., 2008), which we found are approximately twice as stiff along the circumferential axis. However, the isotropic response of *Myxine* skins to tension can be attributed to their fiber angles nearing 45° (Fig. 7). Welsch et al. (1998) also reported fiber angles approximating 45° in *Myxine* skin samples. Furthermore, 45° fiber angles provide the most resistance to maximal tensile stresses applied to hagfish skin during the rapid spinning movements that usually occur immediately before knotting (see Hebrank, 1980). In vivo tensile stress-strain data on hagfish skins are currently absent, however, we can assume that, in the loose-fitting skin of a resting animal, stresses and strains would be minimal. During knotting, they would be considerably

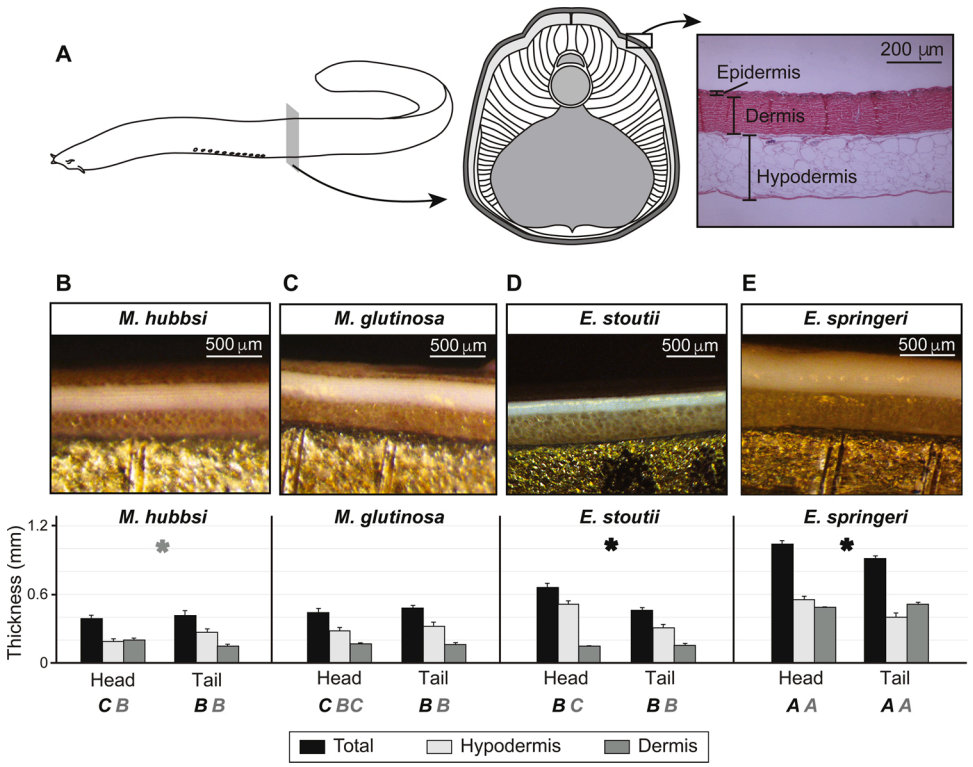

Fig. 6. Morphology of hagfish skins. (A) Left, transverse sections of the body from approximately 50%*TL*. Right, hematoxylin and eosin stained transverse section of a skin sample from *E. stoutii* indicating the three distinct layers: epidermis, dermis, and hypodermis. Modified from Clark et al., 2016. (B) Representative stereomicroscope photograph (above) used for measuring skin layer thicknesses as well as the thickness measurements (below) for *M. hubbsi*, (C) *M. glutinosa*, (D) *E. stoutii*, and (E) *E. springeri*. All data are shown as mean ± s.e.m. Asterisks above the graphs are color-coded for total thickness (black) and dermis thickness (gray) represent significant differences between head and tail regions within a species. Species data not sharing the same capital letters in black or gray (below the graphs) are significantly different.

Table 3
Differences in the total skin thickness and the dermal thickness associated with the effects of all hagfish species and the location on the body (head or tail). *Post hoc* comparisons of thickness between hagfish species and between head and tail regions are included below. *P*-values < 0.05 are in bold text.

	Total Skin Thickness		Dermal Thickness	
All hagfishes	F	*p*	F	*p*
Species	48.706	**< 0.0001**	77.445	**< 0.0001**
Location	2.635	0.115	1.618	0.213
Sp x Loc	4.653	**0.009**	2.169	0.112

Dermal Thickness (head):

Group Comparison		Difference	SE	Lower CL	Upper CL	*P*-value
E. springeri	*E. stoutii*	0.34	0.02	0.29	0.39	**< 0.0001**
E. springeri	*M. glutinosa*	0.32	0.02	0.27	0.38	**< 0.0001**
E. springeri	*M. hubbsi*	0.29	0.02	0.24	0.34	**< 0.0001**
M. hubbsi	*E. stoutii*	0.05	0.02	0.01	0.09	**0.0131**
M. hubbsi	*M. glutinosa*	0.04	0.02	−0.004	0.08	0.0871
M. glutinosa	*E. stoutii*	0.01	0.02	−0.03	0.06	0.7775

Dermal Thickness (tail):

Group Comparison		Difference	SE	Lower CL	Upper CL	*P*-value
E. springeri	*M. hubbsi*	0.36	0.03	0.29	0.44	**< 0.0001**
E. springeri	*E. stoutii*	0.36	0.03	0.28	0.44	**< 0.0001**
E. springeri	*M. glutinosa*	0.36	0.03	0.28	0.43	**< 0.0001**
M. glutinosa	*M. hubbsi*	0.01	0.02	−0.06	0.07	0.9844
M. glutinosa	*E. stoutii*	0.004	0.02	−0.06	0.07	0.9977
E. stoutii	*M. hubbsi*	0.004	0.02	−0.06	0.07	0.9984

	Dermal Thickness (mm)			Total Thickness (mm)		
Species	Head	Tail	*P*-value	Head	Tail	*P*-value
M. hubbsi	0.202±0.014	0.151±0.012	**0.0181**	0.392±0.030	0.418±0.038	0.6014
M. glutinosa	0.164±0.002	0.159±0.016	0.7407	0.441±0.033	0.481±0.024	0.3559
E. stoutii	0.150±0.008	0.155±0.018	0.8152	0.667±0.018	0.464±0.018	**0.0009**
E. springeri	0.449±0.018	0.515±0.022	0.4083	1.045±0.040	0.919±0.045	0.1028

Post hoc tests:
Multiple comparisons of log-transformed skin thickness data from all hagfish species using Tukey-Kramer Honest Significance Tests. *P*-values < 0.05 are in bold text.
T-test results comparing dermal and total thickness between head and tail regions per hagfish species. Data are means ± s.e.m. *P*-values < 0.025 are in bold text.

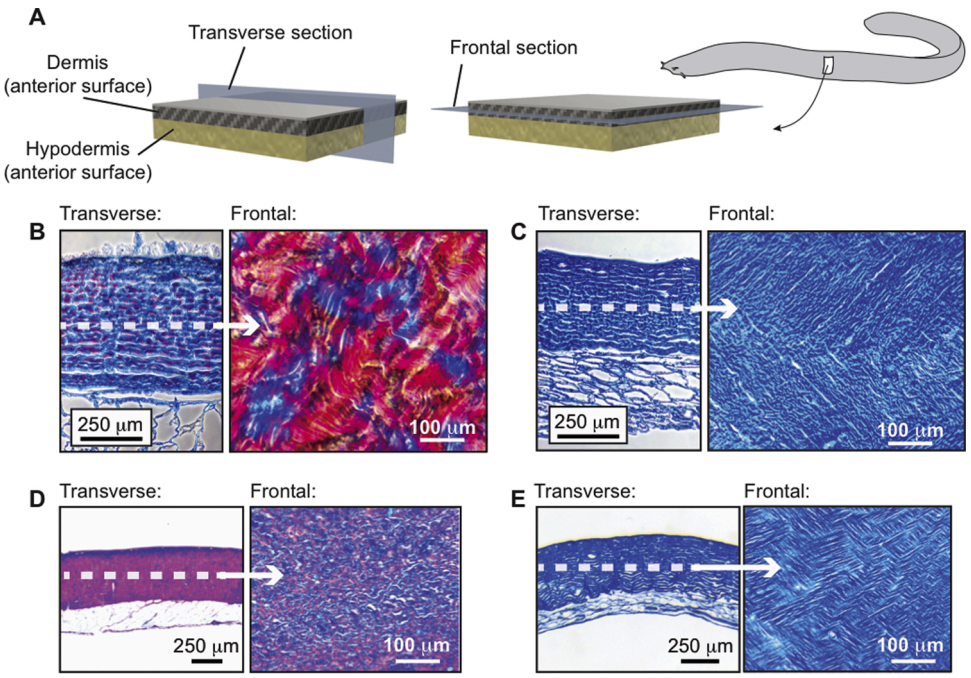

Fig. 7. Histology of hagfish skins. (A) Three-dimensional schematics showing the two anatomical planes, transverse and frontal, from which histological samples were sectioned. (B) Transverse (left) and frontal (right) histological sections of skins dissected from *E. stoutii*, (C) *M. glutinosa*, (D) *E. springeri*, and (E) *M. hubbsi*. The modified Milligan's trichrome stains typically distinguish muscle fibers (magenta) from connective tissue fibers (blue).

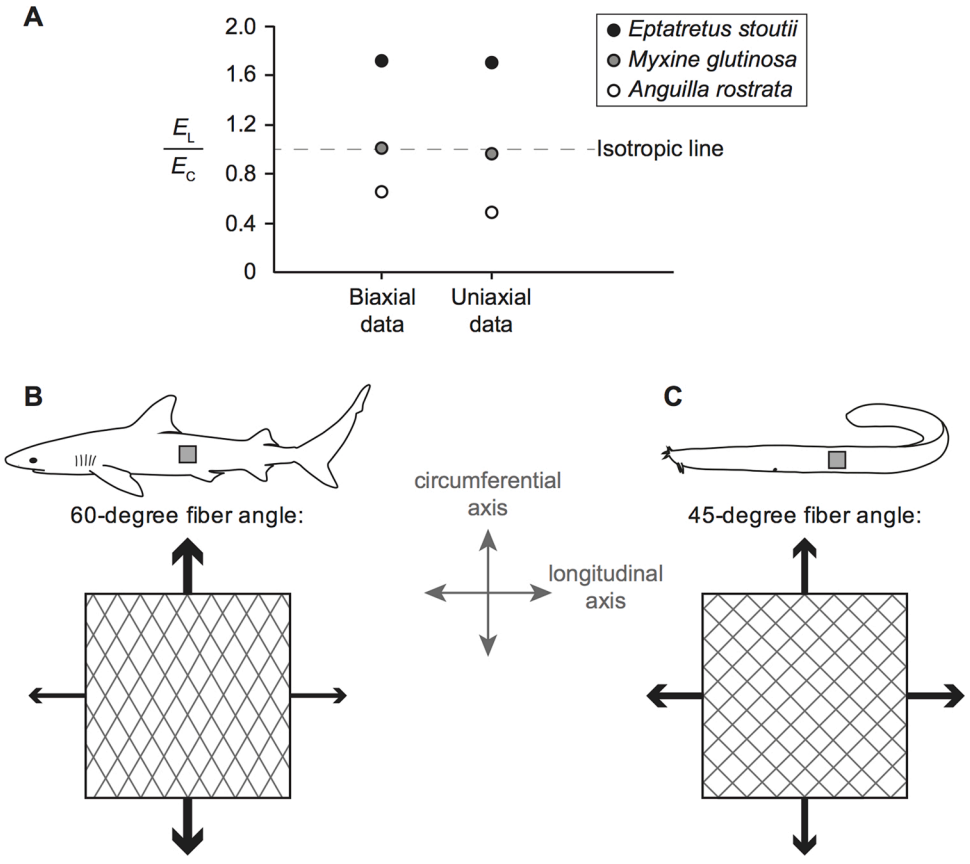

Fig. 8. Illustrating the mechanical behavior of fish skins under tension. (A) Ratios for longitudinal stiffness (E_L) to circumferential stiffness (E_C) in *M. glutinosa, E. stoutii,* and *A. rostrata* determined from biaxial testing methods and uniaxial testing methods plotted relative to the dotted line representing isotropy (E_L:E_C = 1.0). (B) Schematic diagram of the mechanical behavior of a shark skin sample bearing a 60° fiber orientation (this value falls within the range of fiber angles reported by Naresh et al., 1997). The thickness of the arrows indicates the relative magnitudes of tensile loads applied along the longitudinal and circumferential axes. (C) Schematic diagram of the mechanical behavior of a skin sampled from *Myxine* bearing a 45° fiber orientation. Equally thick arrows along both axes illustrate isotropy in the skins of *Myxine*.

higher at regions of the body comprising the body knot.

We also noted that, in contrast to American eels, the mean stiffness of biaxially-strained skins of both species of hagfishes were smaller in magnitude than the mean stiffness gathered from uniaxial testing methods. The higher stiffness of uniaxially-strained samples can be attributed to the lateral narrowing of the unstrained orthogonal axis, which pulls the fibers to reorient along the axis of applied tension to create an additional stiffening effect at higher strains (Mauri et al., 2013). However, previous studies showed that rabbit skins (Lanir and Fung, 1974), porcine aorta (Lally et al., 2004), and human sclera (Eilaghi et al., 2010) were stiffer under biaxial tension but these authors did not provide explanations for their results. The lower stiffness under biaxial tension observed in *M. glutinosa* and *E. stoutii* skins is perplexing. Even though we cannot provide a clear explanation for this result, this study, along with previous work (Clark et al., 2016), demonstrate that hagfish skins respond differently to uniaxial tension than other fish skins and thus may also respond differently to biaxial tension. More biaxial data from the skins of hagfishes, cartilaginous fishes, and bony fish skins are needed for confirmation.

To the authors' best knowledge, loose-fitting isotropic and circumferentially compliant skins like those of hagfishes have not been recorded in the skins of other fish species. Though we have some understanding as to how a hagfish benefits from its baggy skin (Clark et al., 2016; Freedman and Fudge, 2017; Boggett et al., 2017; Uyeno and Clark, 2020), the functional benefits of possessing skins that are equally stiff to significantly stiffer in the longitudinal axis are unclear. One possibility is that circumferentially compliant skins can facilitate knotting by permitting the torsional movements necessary for initiating and manipulating the knot (Clark et al., 2016). During knotting maneuvers, twisting of the body is coupled with high-curvature bending that would otherwise be limited by the rigid, taut-skinned bodies of other fishes. Axial bending in a knotting hagfish is predominantly lateral (bending left and right) as opposed to dorsoventral (Haney et al., 2020). Therefore, the acute bilateral bending during knot-tying can apply considerable amounts of tensile stress on the longitudinal axis of the convex side of the body, which might necessitate more resistance to strains in the longitudinal direction. Even though hagfishes and moray eels (Miller, 1987; Barley et al., 2016; Malcolm, 2016) appear to be the only groups of fishes known to employ knotting for prey capture, cyclic torsion of the tail (Lauder, 2000; Tytell, 2006) and body (Donatelli et al., 2017) occurs during rectilinear swimming activities in many fishes that do not employ knotting. Many elongate species of fishes possess elliptical cross-sections that are hydrodynamically efficient (Eloy, 2013; van Rees et al., 2013) but warp under torsion. In most fishes, excessive amounts of torsion are resisted by rigid internal skeletons made of bone or cartilage and stiff, tight-fitting skins reinforced with cross-helically arranged fibers. In contrast, hagfish bodies appear to have significant amounts of torsional flexibility, given the absence of a rigid skeleton, the skin's baggy fit, and the skin's relatively low stiffness.

4.2. Diversity in the Morphology of Hagfish Skins

The skins of all species of hagfishes we examined are loose-fitting and comprise the layout previously described in Clark et al. (2016) and Weinrauch et al. (2016): A fibrous dermal layer positioned between a thin, superficial epidermis and a thick hypodermis rich with adipose tissue (Fig. 6). We note significant differences in the thickness of skins across hagfish species, with the greatest total and dermal thicknesses belonging to specimens of *E. springeri*. In addition, the dermal morphologies of *Eptatretus* and *Myxine* are histologically distinct. Using the Milligan's trichrome staining protocol for distinguishing muscle tissue and dense connective tissue (Kier, 1992), we found that the dermises from both species of *Myxine* are almost entirely composed of fibrous tissues that stain blue alike collagen fibers (Fig. 7C, E). In contrast, a considerable amount of dermal fibrous tissues in *Eptatretus* stain magenta like muscle tissue (Fig. 7B, D). An additional histological difference between *Eptatretus* and *Myxine* is the amount of vasculature present in the dermis. Numerous capillaries have been described throughout the dermis of *Eptatretus*, and they possibly function in permitting gas exchange and supplying mucous cells (Potter et al., 1995). The dermises in *Myxine* are less vascularized with significantly fewer capillaries, and, this reduction might be associated with the burrowing behaviors regularly performed by species of *Myxine* (Potter et al., 1995; Weinrauch et al., 2016).

These results initially compelled us to consider the possibility that Eptatretine dermises are capable of generating tension in manners similar to mammalian dermises, which possess skeletal muscles for powering facial expressions (Kim et al., 2012) and smooth muscles (arrector pili muscles) for powering the erection of hairs under the pilomotor reflex arc (Poblet et al., 2002; Song et al., 2007). However, in previous attempts, we were unable to electrically stimulate any contractions or record any electrical activity from these skins as we could with axial muscles (Clark and Uyeno, unpublished). In a recent investigation, hematoxylin and eosin stained sections *E. stoutii* skin failed to detect multiple nuclei characteristic of skeletal muscles (Uyeno and Clark, 2020). Alternatively, if the magenta-stained fibers within the dermis of *Eptatretus* are not contractile, then they likely possess muscle proteins that accept the magenta stain. If this were the case, then it is possible that the proteins may enhance extensibility and or elasticity, as they do for cytoskeletons, electric organs, and spindle cells (Monroy et al., 2012, 2017). This might explain the anisotropy and high extensibility in the skins of *E. stoutii*, which possess fiber angles ranging from 44° to 46°, resembling the isotropic skins of *M. hubbsi* and *M. glutinosa*.

More broadly, it is possible that a dermis comprising these tissues could be an adaptation of the Eptatretinae that enables specimens to execute greater varieties and complexities of knots. *M. glutinosa* are capable of tying simple overhand knots (Haney et al., 2020) with significantly less extensible isotropic skins devoid of fibers that stain like muscle. Overhand knots have been recorded in wild specimens of *Neomyxine*, another representative of the Myxininae, attempting to extricate live prey from burrows (Zintzen et al., 2011). Unfortunately, there are insufficient data on the natural behaviors of *M. hubbsi*, which limits our laboratory observations of knotting styles to those employed by *E. stoutii*, *E. springeri*, and *M. glutinosa* (Haney et al., 2020) and observations of wild *Neomyxine* (Zintzen et al., 2011). Nonetheless, the parallels between dermal morphology, phylogeny, and knotting capabilities of these hagfishes are striking.

4.3. Patterns with Lifestyle and Other Behaviors

There are differences in the behaviors and lifestyles of Eptatretines and Myxinines that may bear some connection with the mechanics of the skin. In addition to employing a greater diversity of knotting styles, hagfishes from the genus *Eptatretus* coil when resting while hagfishes from the genus *Myxine* have only been observed resting in an uncoiled position (Strahan, 1963; Miyashita and Palmer, 2014). In addition to having slack skin, the uncoiled resting state of *Myxine* has been proposed to facilitate their fossorial lifestyle, and the genus itself is considered to be more adapted for burrowing than cramming within crevices (Strahan, 1963; Martini, 1998; Miyashita and Palmer, 2014). Furthermore, *M. glutinosa* specimens have been shown to more readily squeeze through small holes than *E. stoutii* (Freedman and Fudge, 2017). In contrast to the fossorial lifestyles of the Myxinines (Weinrauch et al., 2016), Eptatretines are known for taking on more active lifestyles outside of burrows (Forster, 1990), and comparative research on steady swimming kinematics revealed *E. stoutii* specimens achieving higher mean swimming speeds than *M. glutinosa* (Lim and Winegard, 2015). Species of *Eptatretus* occur in benthic habitats with a variety of sediments ranging from soft to hard, while species of *Myxine* appear to be restricted to soft sediments (Martini, 1998). Unlike the hagfishes obtained from the Pacific Ocean (*E. stoutii* and *M. hubbsi*) and the Atlantic Ocean (*M. glutinosa*), *E. springeri* are known for persisting unharmed in brine

pools in the Gulf of Mexico at salinities exceeding 200 ppt (Martini, 1998; D. Grubbs pers. comm.). Interestingly enough, among all hagfish skins examined, the remarkably thick skins from the Gulf hagfish were the weakest, least stiff, and least tough in our study (Fig. 4).

4.4. Comparisons with Other Fish Skins

Interspecific variation in the material properties and morphologies of the skins is a phenomenon that has been identified in other fishes. Recent comparative studies have shown marked interspecific variation in the skins of four species of sharks (Creager and Porter, 2018) and three species of actinopterygians (Kenaley et al., 2018). Furthermore, intraspecific variation has been noted within individual sharks (Creager and Porter, 2018) and striped bass (Szewciw and Barthelat, 2017). As previously demonstrated in *E. stoutii* (Clark et al., 2016), the range of magnitudes for stiffness and strength in hagfish skins overlaps with that of the taut skins of other fishes. However, our results suggest that this overlap occurs in the lower end of the range of magnitudes for taut fish skins. Here, we report a range of stiffness in hagfish skins nearing one order of magnitude (6 MPa – 58 MPa), a fivefold range in strength (4 MPa – 23 MPa), and a fourfold range in toughness (0.75 MJ m^{-3} – 3 MJ m^{-3}). These values for hagfish skins are significantly smaller than those gathered from the skins of bony fishes and cartilaginous fishes. In the skins of four species of coastal sharks, Creager and Porter (2018) reported a large range of magnitudes for material properties, with the stiffness ranging from 17 MPa to 229 MPa and toughness ranging from 2.5 MJ m^{-3} to 16 MJ m^{-3}. We also noted significantly larger magnitudes for stiffness (116 MPa – 234 MPa), strength (47 MPa – 62 MPa), and toughness (4.6 MJ m^{-3} – 4.8 MJ m^{-3}) in the skins of *A. rostrata* (Fig. 4). Even though the skins of hagfishes appear to fall on the lower end of the spectrum of magnitudes for stiffness, strength, and toughness of many fish skins, they are considerably more extensible in representatives of *Eptatretus*. The peak strains of *E. stoutii* (0.48 $\pm$ 0.03) and *E. springeri* (0.47 $\pm$ 0.09) are significantly larger than those of *Myxine* and *Anguilla,* and approach the extensibilities required to inflate the skins of the pufferfish *Diodon holocanthus* (Brainerd, 1994). However, it is important to note that the stress-strain curves of *Eptatretus* skins comprise shorter and less prominent toe regions than the stress-strain curves of skins from pufferfish, which have conspicuously long toe regions where the skin stretches to 40% of its original length while minimal stress is applied (Brainerd, 1994).

In contrast to the slack skins of hagfishes, the taut skins of many fish taxa are important for steady locomotion. Fish skins function well at transmitting forces due to myoseptal-skin connections (Pabst, 1996; Gemballa et al., 2003; Kenaley et al., 2018) and, in some species of sharks and eels, can function like exotendons (Wainwright et al., 1978; Hebrank, 1980). Previous studies have shown that surgically removing the skins from bony fishes can have significant effects on the body's flexural stiffness (Long et al., 1996; Szewciw and Barthelat, 2017). For example, Long et al. (1996) demonstrated this decrease in flexural stiffness and concomitant increase in tail beat frequencies of the longnose gar(,) *Lepisosteus osseus*. This relationship between the skin and steady swimming kinematics is absent in hagfishes, which theoretically can swim in the absence of their skins (Long et al., 2002). Steady-state locomotion in hagfishes is peculiar as these animals employ a variety of strategies for modulating swimming speeds (Lim and Winegard, 2015), and the swimming hagfish body has a remarkable ability to approach its natural resonance frequency without sustaining injury (Long et al., 2002; Summers and Long, 2006). While apparently useless in steady rectilinear locomotion, the function of hagfish skins (Uyeno and Clark, 2020) becomes more significant when encountering predators (Boggett et al., 2017) or executing unsteady locomotor behaviors like squeezing though narrow openings (Freedman and Fudge, 2017) or tying their bodies into knots (Clark et al., 2016; Haney et al., 2020).

5. Conclusions

In this study, we consider the structure and function of the loose-fitting skins in four hagfish species representing the two major subfamilies within the Myxinidae. There are clear differences in the skins' material properties and morphologies, which fit a pattern reflecting the variation in the knotting kinematics and whole-body resting positions employed by species of *Eptatretus* (subfamily Eptatretinae) and species of *Myxine* (subfamily Myxininae). Skins from *Eptatretus* are highly extensible, anisotropic, and possess fibers that stain like collagen and non-contractile fibers that stain like muscle in the dermis, in contrast to the less extensible, isotropic skins from *Myxine* that possess only fibers that stain like collagen. Relative to *A. rostrata* and previously studied skins from cartilaginous and bony fishes, hagfish skins subjected to quasi-static uniaxial and biaxial tensile tests to failure tend to be more compliant and more extensible but are generally weaker and store less tensile strain energy.

Declaration of Competing Interest

The authors declare that they have no known competing financial interests or personal relationships that could have appeared to influence the work reported in this paper.

Acknowledgements

Caleb Gilbert (NOAA NMFS), Kim Penttila (CA Dept. Fish and Wildlife), Dr. Dean Grubbs (Coastal and Marine Laboratory, Florida State University), Donna Downs (WA Dept. Fish and Wildlife), and the Olympic Coast Seafood Co. (Port Angeles, WA) provided the hagfish specimens. Comments from two anonymous reviewers helped us improve earlier drafts of this manuscript. This research was supported by funding from the National Science Foundation (IOS-1354787 awarded to AJC and TAU) and a CofC MAYS grant to EBLK.

References

Barley, S.C., Mehta, R.S., Meeuwig, J.J., Meekan, M.G., 2016. To knot or not? Novel feeding behaviours in moray eels. Mar. Biodivers. 46, 703–705.
Billingham, R.E., Medawar, P.B., 1951. The technique of free skin grafting in mammals. J. Exp. Biol. 28 (3), 385–402.
Boggett, S., Stiles, J.L., Summers, A.P., Fudge, D.S., 2017. Flaccid skin protects hagfishes from shark bites. J. R. Soc. Interface. 14, 20170765.
Brainerd, E.L., 1994. Pufferfish inflation: functional morphology of postcranial structures in *Diodon holocanthus* (Tetraodontiformes). J. Morphol. 220, 243–261.
Clark, R.B., Cowey, J.B., 1958. Factors controlling the change of shape of certain nemertean and turbellarian worms. J. Exp. Biol. 35, 731–748.
Clark, A.J., Summers, A.P., 2007. Morphology and kinematics of feeding in hagfish: possible functional advantages of jaws. J. Exp. Biol. 210, 3897–3909.
Clark, A.J., Summers, A.P., 2012. Ontogenetic scaling of the morphology and biomechanics of the feeding apparatus in the Pacific hagfish *Eptatretus stoutii*. J. Fish Biol. 80, 86–99.
Clark, A.J., Uyeno, T.A., 2019. Feeding in jawless fishes. In: Bels, V., Whishaw, I.Q. (Eds.), Feeding in Vertebrates – Evolution, Morphology, Behavior, Biomechanics. Springer, New York, pp. 189–230.
Clark, A.J., Maravilla, E.J., Summers, A.P., 2010. A soft origin for a forceful bite: motor patterns of the feeding musculature in Atlantic hagfish, *Myxine glutinosa*. Zoology. 113, 259–268.
Clark, A.J., Crawford, C.H., King, B.D., Demas, A.M., Uyeno, T.A., 2016. Material properties of hagfish skin, with insights into knotting behaviors. Biol. Bull. 230, 243–256.
Clubb, B.L., Clark, A.J., Uyeno, T.A., 2019. Powering the hagfish "bite": The functional morphology of the retractor complex of two hagfish feeding apparatuses. J. Morphol. 280, 827–840.
Creager, S.B., Porter, M.E., 2018. Stiff and tough: a comparative study on the tensile properties of shark skin. Zoology. 126, 154–163.
Danos, N., Fisch, N., Gemballa, S., 2008. The musculotendinous system of an anguilliform swimmer: muscles, myosepta, dermis, and their interconnections in *Anguilla rostrata*. J. Morphol. 269, 29–44.
Donatelli, C.M., Summers, A.P., Tytell, E.D., 2017. Long-axis twisting during locomotion of elongate fishes. J. Exp. Biol. 220, 3632–3640.
Eilaghi, A., Flanagan, J.G., Tertinegg, I., Simmons, C.A., Brodland, G.W., Ethier, C.R., 2010. Biaxial mechanical testing of human sclera. J. Biomech. 43, 1696–1701.
Eloy, C., 2013. On the best design for undulatory swimming. J. Fluid Mech. 717, 48–89.

Fernholm, B., Norén, M., Kullander, S.O., Quattrini, A.M., Zintzen, V., Roberts, C.D., Mok, H.K., Kuo, C.H., 2013. Hagfish phylogeny and taxonomy, with description of the newgenus *Rubicundus* (Craniata, Myxinidae). J. Zool. Syst. Evol. Res. 51, 296–307.
Forster, M.E., 1990. Confirmation of the low metabolic rate of hagfish. Comp. Biochem. Physiol. A. 96, 113–116.
Forster, M.E., Davison, W., Satchell, G.H., Taylor, H.H., 1989. The subcutaneous sinus of the hagfish, *Eptatretus cirrhatus* and its relation to the central circulating blood volume. Comp. Biochem. Physiol. Part A Physiol. 93, 607–612.
Forster, M.E., Axelsson, M., Farrell, A.P., Nilsson, S., 1991. Cardiac function and circulation in hagfishes. Can. J. Zool. 69, 1985–1992.
Freedman, C.R., Fudge, D.S., 2017. Hagfish Houdinis: biomechanics and behavior of squeezing through small openings. J. Exp. Biol. 220, 822–827.
Gemballa, S., Ebmeyer, L., Hagen, K., Hannich, T., Hoja, K., Rolf, M., Treiber, K., Vogel, F., Weitbrecht, G., 2003. Evolutionary transformations of myoseptal tendons ingnathostomes. Proc. R. Soc. London B. 270, 1229–1235.
Grear, M.E., Motley, M.R., Crofts, S.B., Witt, A.E., Summers, A.P., Ditsche, P., 2018. Mechanical properties of harbor seal skin and blubber - a test of anisotropy. Zoology. 126, 137–144.
Gustafson, G., 1935. On the biology of *Myxine glutinosa*. Ark. Zool. 28A, 1–8.
Haney, W.A., Clark, A.J., Uyeno, T.A., 2020. Characterization of body knotting behavior used for escape in a diversity of hagfishes. J. Zool. 310, 261–272.
Hebrank, M.R., 1980. Mechanical properties and locomotor functions of eel skin. Biol. Bull. 158, 58–68.
Hebrank, M.R., Hebrank, J.H., 1986. The mechanics of fish skin: lack of an "external tendon" role in two teleosts. Biol. Bull. 171, 236–247.
Helfman, G.S., Clark, J.B., 1986. Rotational feeding: overcoming gape-limited foraging inanguillid eels. Copeia. 1986, 679–685.
Horton, J.M., Drucker, E.G., Summers, A.P., 2004. Swiftly swimming fish show evidence of stiff spines. Integ. Comp. Zool. 43, 905.
Jensen, D., 1966. The hagfish. Sci. Am. 214, 82–91.
Kenaley, C.P., Sanin, A., Ackerman, J., Yoo, J., Alberts, A., 2018. Skin stiffness in ray-finned fishes: contrasting material properties between species and body regions. J. Morphol. 279, 1419–1430.
Kier, W.M., 1992. Hydrostatic skeletons and muscular hydrostats. In: Biewener, A.A. (Ed.), Biomechanics (Structures and Systems): A Practical Approach. Oxford University Press, Oxford, pp. 205–231.
Kim, J.N., Lee, J.Y., Yoo, J.Y., Paik, D.J., Koh, K.S., Song, W.C., 2012. The morphology and origin of the skeletal muscle bundles associated with the human mustache. Anat. Sci. Int. 87, 132–135.
Lally, C., Reid, A.J., Prendergast, P.J., 2004. Elastic behavior of porcine coronary artery tissue under uniaxial and equibiaxial tension. Ann. Biomed. Eng. 32, 1355–1364.
Lanir, Y., Fung, Y.C., 1974. Two-dimensional mechanical properties of rabbit skin—II. Experimental results. J. Biomech. 7 (2), 171–182.
Lauder, G.V., 2000. Function of the caudal fin during locomotion in fishes: kinematics, flow visualization, and evolutionary patterns. Am. Zool. 40, 101–122.
Lim, J.L., Winegard, T.M., 2015. Diverse anguilliform swimming kinematics in Pacific hagfish (*Eptatretus stoutii*) and Atlantic hagfish (*Myxine glutinosa*). Can. J. Zool. 93, 213–223.
Long, J., Hale, M., McHenry, M., Westneat, M., 1996. Functions of fish skin: flexural stiffness and steady swimming of longnose gar, *Lepisosteus osseus*. J. Exp. Biol. 199, 2139–2151.
Long Jr., J.H., Koobs-Emunds, M., Sinwell, B., Koob, T.J., 2002. The notochord of hagfish, *Myxine glutinosa*: viscoelastic properties and mechanical function during steady swimming. J. Exp. Biol. 205, 3819–3831.
Malcolm, H.A., 2016. A moray's many knots: knot tying behaviour around bait in two species of *Gymnothorax* moray eel. Environ. Biol. Fishes. 99, 939–947.
Martinez, G., Drucker, E.G., Summers, A.P., 2003. Under pressure to swim fast. Integ. Comp. Biol. 42, 1273–1274.
Martini, F.H., 1998. The ecology of hagfishes. In: Jørgensen, J.M., Lomholt, J.P., Weber, R.E., Malte, H. (Eds.), The Biology of Hagfishes. Chapman and Hall, London, pp. 57–77.
Mauri, A., Zeisberger, S.M., Hoerstrup, S.P., Mazza, E., 2013. Analysis of the uniaxial and multiaxial mechanical response of a tissue-engineered vascular graft. Tissue Eng. Part A. 19, 583–592.
Micozzi, M.S., 1986. Experimental study of postmortem change under field conditions: effects of freezing, thawing, and mechanical injury. J Forensic Sci. 31, 953–961.
Miller, T.J., 1987. Knotting: a previously undescribed feeding behavior in muraenid eels. Copeia. 1987, 1055–1057.
Miyashita, T., Palmer, A.R., 2014. Handed behavior in hagfish – an ancient vertebrate lineage – and a survey of lateralized behaviors in other invertebrate chordates and elongate vertebrates. Biol. Bull. 226, 111–120.
Monroy, J.A., Powers, K.L., Gilmore, L.A., Uyeno, T.A., Lindstedt, S.L., Nishikawa, K.C., 2012. What is the role of titin in active muscle? Exerc. Sport Sci. Rev. 40, 73–78.
Monroy, J.A., Powers, K.L., Pace, C.M., Uyeno, T., Nishikawa, K.C., 2017. Effects of activation on the elastic properties of intact soleus muscles with a deletion in titin. J. Exp. Biol. 220, 828–836.
Motta, P.J., 1977. Anatomy and functional morphology of dermal collagen fibers insharks. Copeia. 1977, 454–464.
Naresh, M.D., Arumugam, V., Sanjeevi, R., 1997. Mechanical behaviour of sharkskin. J. Biosci. 22, 431–437.
Pabst, D.A., 1996. Springs in swimming animals. Am. Zool. 36, 723–735.
Poblet, E., Ortega, F., Jiménez, F., 2002. The arrector pili muscle and the follicular unit of the scalp: a microscopic anatomy study. Dermatol. Surg. 28, 800–803.
Potter, I.C., Welsch, U., Wright, G.M., Honma, Y., Chiba, A., 1995. Light and electron microscope studies of the dermal capillaries in three species of hagfishes and three species of lampreys. J Zool. 235, 677–688.
Ranamukhaarachchi, S.A., Lehnert, S., Ranamukhaarachchi, S.L., Sprenger, L., Schneider, T., Mansoor, I., Rai, K., Häfeli, U.O., Stoeber, B., 2016. A micromechanical comparison of human and porcine skin before and after preservation by freezing for medical device development. Sci Rep. 6, 32074.
Rasband, W.S., 1997. ImageJ.
Song, W.C., Hu, K.S., Kim, H.J., Koh, K.S., 2007. A study of the secretion mechanism of these baceous gland using three-dimensional reconstruction to examine the morphological relationship between the sebaceous gland and the arrector pili muscle in the follicular unit. Br. J. Dermatol. 157, 325–330.
Strahan, R., 1963. The behavior of myxinoids. Acta. Zool. 44, 1–30.
Summers, A.P., Long Jr., J.H., 2006. Skin and bones, sinew and gristle: the mechanical behavior of fish skeletal tissues. In: Shadwick, R.E., Lauder, G.V. (Eds.), Fish Biomechanics. Elsevier, Amsterdam, pp. 141–177.
Szewciw, L., Barthelat, F., 2017. Mechanical properties of striped bass fish skin: Evidence of anexotendon function of the stratum compactum. J. Mech. Behav. Biomed. Mater. 73, 28–37.
Tytell, E.D., 2006. Median fin function in bluegill sunfish, *Lepomis macrochirus*: Stream wise vortex structure during steady swimming. J. Exp. Biol. 209, 1516–1534.
Uyeno, T.A., Clark, A.J., 2015. Muscle articulations: flexible jaw joints made of soft tissues. Integr. Comp. Biol. 55, 193–204.
Uyeno, T.A., Clark, A.J., 2020. On the fit of skins with a particular focus on the biomechanics of loose skins of hagfishes. Can. J. Zool. https://doi.org/10.1139/cjz-2019-0296.
van Rees, W.M., Gazzola, M., Koumoutsakos, P., 2013. Optimal shapes for anguilliform swimmers at intermediate Reynolds numbers. J. Fluid. Mech. 722, 1–12.
Vogel, S., 2013. Comparative Biomechanics: Life's Physical World. Princeton University Press, Princeton.
Vogel, F., Gemballa, S., 2000. Locomotory design of 'cyclostome' fishes: spatial arrangement and architecture of myosepta and lamellae. Acta Zool. 81, 267–283.
Wainwright, S.A., Vosburgh, F., Hebrank, J.H., 1978. Shark skin: function in locomotion. Science. 202, 747–749.
Waldman, S.D., Lee, J.M., 2005. Effect of sample geometry on the apparent biaxial mechanical behaviour of planar connective tissues. Biomaterials. 26, 7504–7513.
Weinrauch, A.M., Edwards, S.L., Goss, G.G., 2016. Anatomy of the Pacific hagfish (*Eptatretus stoutii*). In: Edwards, S.L., Goss, G.G. (Eds.), Hagfish biology. CRC Press, Boca Raton, pp. 1–39.
Welsch, U., Büchl, S., Erlinger, R., 1998. The dermis. In: Jørgensen, J.M., Lomholt, J.P., Weber, R.E., Malte, H. (Eds.), The Biology of Hagfishes. Chapman and Hall, London, pp. 133–142.
Zintzen, V., Roberts, C.D., Anderson, M.J., Stewart, A.L., Struthers, C.D., Harvey, E.S., 2011. Hagfish predatory behaviour and slime defense mechanism. Sci. Rep. 1, 1–6.